Sea-Surface Drift Currents Induced by Wind and Waves

JIN WU

College of Marine Studies, University of Delaware, Newark, DE 19711

ABSTRACT

Wind-induced shear currents and wave-induced mass transports at various fetches of both clean and slick sea surfaces are separately estimated. At the clean surface, the ratio between wind-induced current and wind velocity decreases, while the ratio between wave-induced current and wind velocity increases, with increasing fetch. The total surface drift current, the sum of wind- and wave-induced components, decreases gradually with increasing fetch and approaches 3.1% of wind velocity at long fetches, comparing very favorably with measured values. At a slick surface, the wind-induced drift current is reduced due to a decrease of the wind-stress coefficient, and the wave-induced mass transport is increased due to an additional wave damping. As a result of these opposite effects, the total surface drift current at a slick surface differs much less significantly than individual components from that at a clean surface. It is also suggested that the surface mass transport can be calculated simply from characteristics of dominant waves and that discrepancy between earlier measured currents of clean and slick surfaces is due to a direct momentum flux from wind to waves. Finally, linear superposition of wind- and wave-induced components and effects of water depth on surface drift currents are discussed.

1. Introduction

Drift currents near the sea surface affect momentum, heat, and mass transfers across the air-water interface, and consequently, influence physical, chemical, and biological processes within the upper ocean and the atmospheric surface layer. As for practical interests, drift currents govern dispersion of man-made discharges near the sea surface, and influence design, deployment, and stability of offshore structures. On the basis of scaling law of wind-stress coefficients (Wu, 1969a), wave data at various fetches (Wiegel, 1964), and laboratory measurements of drift currents (Wu, 1975), an estimate by Wu (1975) was presented of sea-surface drift currents consisting of wind- and wave-induced components of all fetches under various wind velocities.

Previous estimates of wind-induced surface drift currents (Wu, 1975) are refined by taking into account the partition of wind stress between momentum fluxes to currents and to waves. It is also suggested that wave-induced drift currents (Stokes mass transports) at the sea surface can be calculated as accurately with average characteristics of dominant waves as from a wave spectrum. The estimated total surface drift currents agree well with other laboratory (Lange and Hühnerfuss, 1978) and oceanic (Hughes, 1956; Smith, 1968) data. Further comparisons between present estimates and results from other investigations also uncover several features of their measurements, such as effects of wave drag on producing drift currents and validity of linear superposition of wind- and wave-induced components. The mass transport of waves under a slick surface is greater than that under a clean surface due to dynamic interactions between the surface film and waves. On the other hand, the wind-stress coefficient of a slick surface is smaller than that of a clean surface, resulting in a smaller wind-induced drift current under the slick surface. Available laboratory results (Alofs and Reisbig, 1972) on slick movements and field results (Barger et al., 1970) on wind structures over slicks are reanalyzed to provide the basis for estimating movements of slicks of various sizes over waves of different lengths under various wind velocities.

2. Drift currents of clean surface

The clean surface is referred to here as the surface free of either man-made or natural slicks.

a. Experiments in laboratories

1) SURFACE MASS TRANSPORT OF GRAVITY WAVES

A slow but steady forward motion of water particles under surface waves was theoretically predicted by Stokes (1847). The so-called Stokes transport at the water surface V_v can be expressed as

$$V_v = \sigma a^2 k, \tag{1}$$

where σ, a, and k are the radian frequency, amplitude, and wavenumber of waves, respectively. The best ver-

ification of the above expression was provided by Lange and Hühnerfuss (1978); see Fig. 1a, in which the measured current is plotted versus the value calculated from (1). It is noted that although Lange and Hühnerfuss's experiments were performed with monolayers, the latter to be further discussed showed no streaming effects.

2) SURFACE DRIFT CURRENT OF WIND WAVES

The drift current of a wind-disturbed water surface has two components: wind-induced shear current and wave-induced mass transport. Studies on drift currents in a wind-wave tank have been conducted, among others, by Wu (1975). The drift currents in the upper 3 mm were measured by timing spherical floats of different sizes passing two stations along the tank. The measured velocity was considered as the current at a depth of the centroid of longitudinally projected area of the submerged portion of the float. The surface drift current was determined by extrapolating the current-distribution curve to the water surface. In the same study, the Stokes surface transport was estimated from (1) with average height and length of dominant waves. It was found that due to

a limited wave growth, the Stokes transport in laboratory tanks was only about ⅛ of the total surface drift current; see Fig. 1b, where V is the total surface drift current, and U the maximum wind velocity in the tunnel.

The difference between measured total drift current and estimated Stokes transport was considered as the wind-induced current. The wind-friction velocity was suggested as the proper parameter for correlating this component (Wu, 1975). No systematic variation of the ratio between this component and wind-friction velocity with the wind velocity was found. The results shown in Fig. 2a obey roughly

$$\frac{V_n}{u_{*_a}} = 0.53, \tag{2}$$

where V_n is the wind-induced surface drift current; u_{*_a} is the wind-friction velocity, $u_{*_a} = (\tau/\rho_a)^{1/2}$ in which τ is the wind stress and ρ_a the air density.

Growing with both wind velocity and fetch, waves increase their momentum and extract a portion of the momentum flux from the wind. As a result of this direct momentum flux to waves, the so-called wave drag (Stewart, 1961), only a portion of the momentum flux from the wind is used to produce drift currents (Lighthill, 1971). Consequently, the shear stress applied by currents on the underside of the air–water interface is smaller than the wind stress applied on the upperside: $\rho_w u_{*_w}^2 < \rho_a u_{*_a}^2$, where ρ_w is the density of water and u_{*_w} the friction velocity of currents. Obtained from Wu (1975), the ratios between the wind-induced surface current and the current-friction velocity are presented in Fig. 2b. The variation shown in the figure, as in Fig. 2a, appears to be related to wave breaking; it suffices for the present study to use an average ratio,
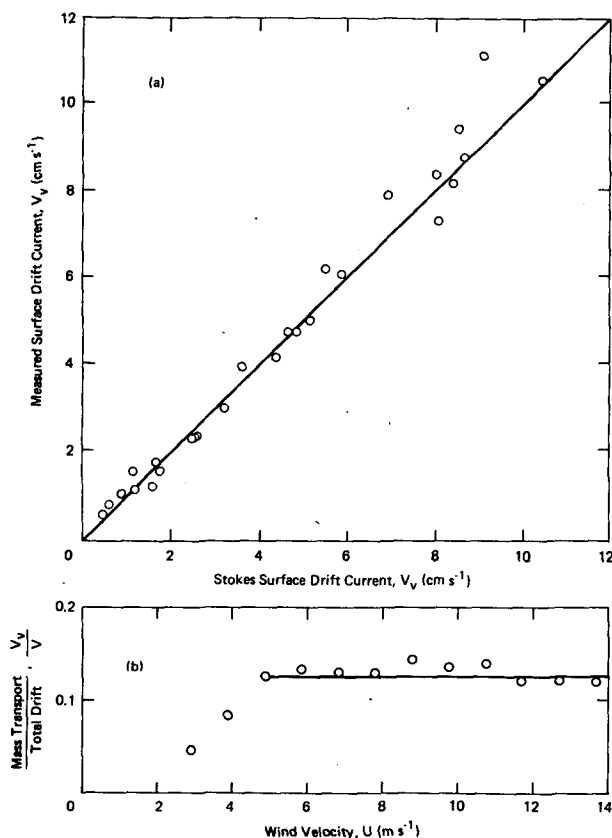
$$\frac{V_n}{u_{*_w}} = 22. \tag{3}$$

FIG. 1. Laboratory results of wave-induced surface mass transport (a) without (Lange and Hühnerfuss, 1978) and (b) with (Wu, 1975) wind.

If the shear stress were continuous across the air–water interface, we should have from (2): $V_n/u_{*_w} = 0.53(\rho_w/\rho_a)^{1/2} = 15.2$.

Earlier laboratory results of surface drift currents (Keulegan, 1951; Wu, 1968) were compiled by Wu (1973). These earlier data along with other results (Baines and Knapp, 1965; Shemdin, 1972; Wu, 1975) are presented in Fig. 2c. The surface drift currents are seen to increase very rapidly with the wind velocity around $u_{*_a} = 20$ cm s⁻¹. The data for $u_{*_a} > 20$ cm s⁻¹ were averaged by first dividing the friction velocity into bands of 10 cm s⁻¹ and then averaging the data sorted into each band. The results shown in Fig. 2d have no obvious systematic dependence upon the wind–friction velocity, and are seen to be reasonably well approximated by
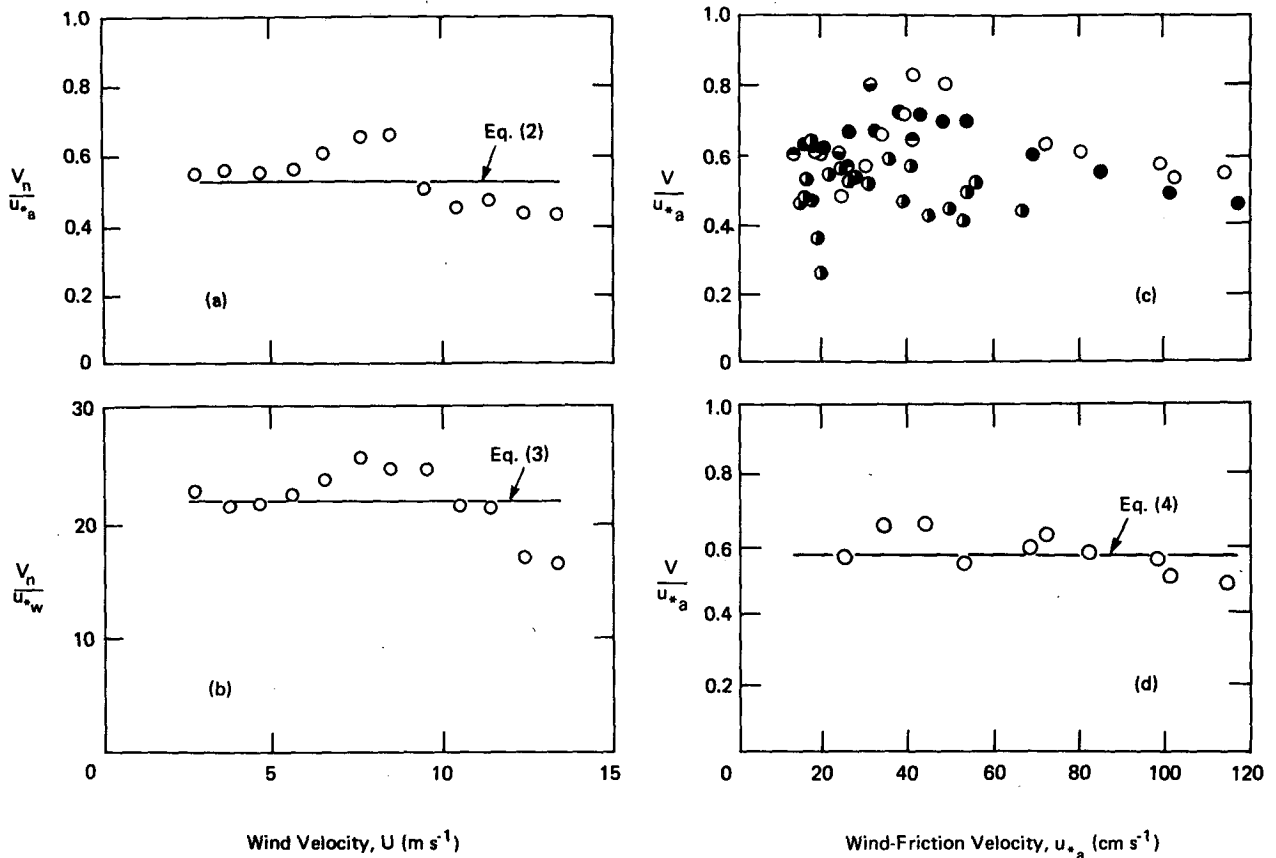
$$\frac{V}{u_{*_a}} = 0.57. \tag{4}$$

FIG. 2. Laboratory results of (a, b) wind-induced surface drift currents (Wu, 1975), (c) total surface drift currents measured by Keulegan (1951) right half solid, Baines and Knapp (1965) top half solid, Wu (1968) open circle, Shemdin (1972) bottom half solid, and Wu (1975) solid circle and (d) averaged results from above data.

There is no significant discrepancy between (2) for the wind-induced surface drift current and (4) for the total surface drift current, as the Stokes surface transport in laboratory tanks is, in most cases as shown in Fig. 1b, only about ⅛ the total surface drift current.

b. Estimations for field

1) ESTIMATIONS OF MASS TRANSPORT FROM WAVE SPECTRUM AND FROM DOMINANT WAVES

The Stokes mass transport at the sea surface can be calculated from a wave spectrum (Bye, 1967) as

$$V_v = \frac{2}{g} \int_0^\infty \Phi(\sigma)\sigma^3 d\sigma, \qquad (5)$$

where g is the gravitational acceleration, and $\Phi(\sigma)$ the frequency spectrum of ocean waves. In this calculation, the wave component at each frequency is considered to contribute to the surface mass transport according to (1) weighed by its energy density, $V_v \sim \Phi(\sigma)\sigma^3$.

The spectrum of ocean waves has a skewed bell shape. Wave components on the low-frequency side

of the spectral peak are far from saturated; their energy density decreases very rapidly from the spectral peak. The contribution of these wave components to the mass transport, therefore, diminishes even much more rapidly toward the low-frequency end because their contribution as discussed above is weighed with not only their energy density but also the cube of their frequency. Owing to exactly this reason, the low-frequency side of the spectrum was left out in most calculations of the mass transport from the spectrum (Bye, 1967).

The wave components on the high-frequency side of the spectral peak are fully saturated, and their energy density can be described by the equilibrium spectrum (Phillips, 1977) as

$$\Phi(\sigma) = \beta g^2 \sigma^{-5}, \qquad (6)$$

where β is the spectral coefficient. Consequently, for the high-frequency side, we have from (6),

$$V_v \sim (\sigma^{-5})\sigma^3 \sim \sigma^{-2}. \qquad (7)$$

The contribution to mass transport from wave components on the high-frequency side thus also de-

creases very rapidly toward the high-frequency end away from the spectral peak.

In summary, contributions to the Stokes surface current from various wave components decrease very rapidly from the spectral peak toward both low- and high-frequency ends of the spectrum. In order to illustrate relative contributions of various wave components, a sample wave spectrum from the JONSWAP Project cited in (Hasselmann, *et al.*, 1976, Fig. 1a) is reproduced as a dashed line in Fig. 3, where f is the wave frequency. The integrand in (5) was first calculated from the spectrum and then normalized with respect to its maximum value. Plotted as a solid line in Fig. 3, the integrand (I) is seen to be negligible on the low-frequency side of the spectral peak and to be much greater within a very narrow band around the frequency of dominant waves than those on the high-frequency side. Furthermore, the energy densities of wave components with $f > 0.15$ Hz are seen to be beyond the sharp dropoff; the results at these high frequencies were probably less certain, as the measurements were performed very close to the noise range of the instrument. Moreover, recent discussion on modulations of ripples by long waves (Phillips, 1977, 4.4) also casts doubt on the use of (5) neglecting all interaction terms. In other words, contributions to the Stokes drift current at the sea surface appear to come mainly from dominant waves. The surface mass transport calculated rather simply from the av-

erage characteristics of dominant waves should provide as reliable an estimation as that calculated from the wave spectrum.

2) ESTIMATION OF PROBABLE SURFACE DRIFT CURRENTS

As indicated above, the surface drift current has two components: the wind-induced component generated by the wind stress and the wave-induced component related to wave characteristics. Therefore, in order to determine total surface drift currents at various fetches, both components must be first estimated separately, on the basis of respective scaling laws, and then summed to determine the total surface drift current. Such an estimation made earlier (Wu, 1973, 1975) is refined here by including the direct momentum flux from wind to waves and by adopting a newly determined Charnock constant.

A nondimensional expression for determining wind-stress coefficients at various fetches has been established by Wu (1969a):

$$1/C_z^{1/2} = 2.5 \ln(1/aC_zF^2), \quad F = U_z/(gz)^{1/2}, \quad (8)$$

where $a = 0.0185$ is the Charnock constant (Wu, 1980), F the Froude number, $C_z = \tau/(\rho_a U_z^2)$ the wind-stress coefficient, and U_z the wind velocity at an elevation z above the mean water surface. Staying within the constant-flux layer, the anemometer height was proposed as (Wu, 1971)

$$z = 7.35 \times R^{2/3} \times 10^{-7} \text{ m}, \quad (9)$$

where $R = U_z L/\nu_a$ is the fetch Reynolds number, L the wind fetch, and ν_a the kinematic viscosity of air.

Wave data for various wind velocities and fetches were compiled by Wiegel (1964) and fitted (Wu, 1969b) with the following expressions

$$c/U_z = 0.05(gL/U_z^2)^{0.3} \\ gH_{1/3}^2/U_z^2 = 0.00305(gL/U_z^2)^{0.465} \Big\}, \quad (10)$$

where c and $H_{1/3}$ are the phase velocity and height of dominant (significant) waves, respectively. The momentum of wind waves can be approximated by that for irrotational waves

$$M = \frac{E}{c} = \frac{1}{8} \rho_w g H_{1/3}^2 c^{-1}, \quad (11)$$

where M and E are momentum and energy of waves per unit area of the water surface, respectively. The coefficient of wave drag (C_v), representing the portion of the wind stress consumed to support the increase of wave momentum in the wind direction (x-axis), can be estimated from (10) and (11) by

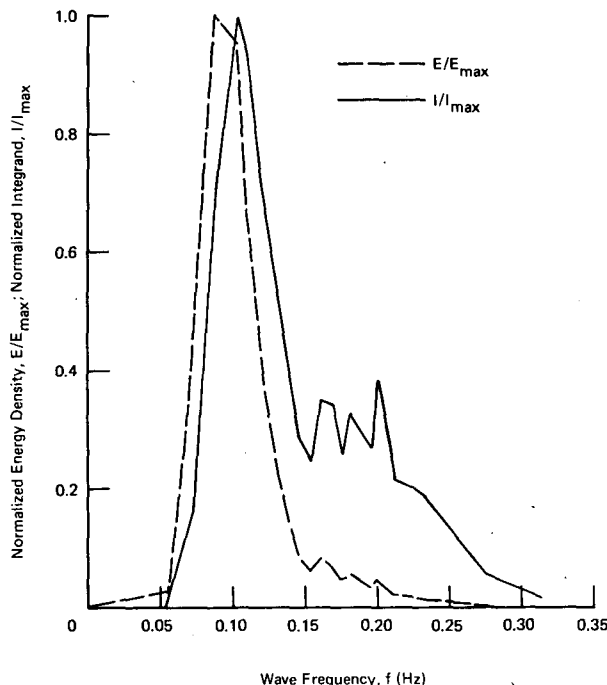$$C_v = c \frac{dM}{dx} (\rho_a U_z^2)^{-1} = 6.3(gLU_z^{-2})^{-0.07} \times 10^{-4}. \quad (12)$$

FIG. 3. Relative contributions of various wave components to surface mass transport. The wave spectrum is from the JONSWAP Project [Hasselmann *et al.*, 1973].
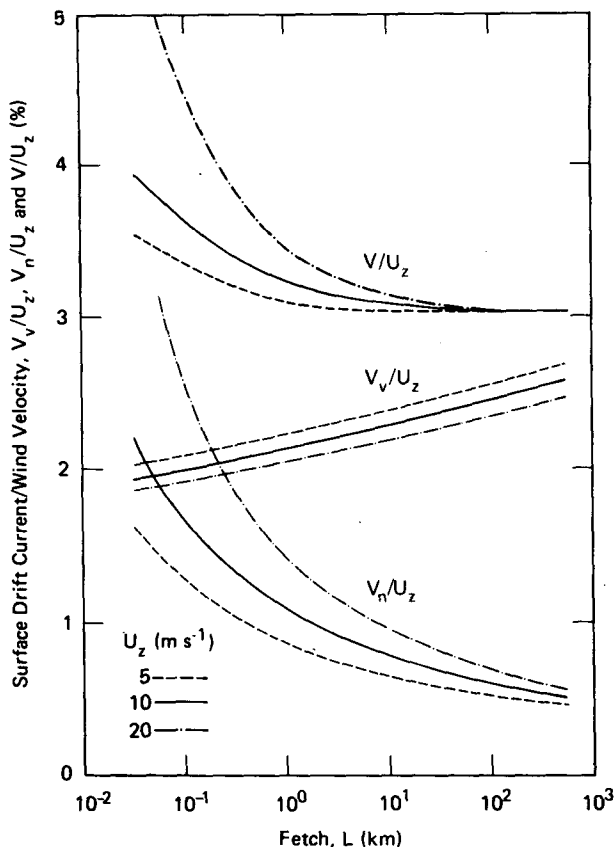
FIG. 4. Wind-induced (V_n) and wave-induced (V_v) surface drift currents and total (V) surface drift currents.

Combining (8) and (9), the wind-stress coefficients can be determined; subsequently, along with (12), the friction velocity of currents can be obtained from

$$u_{*_w} = (C_z - C_v)^{1/2} U_z \left(\frac{\rho_a}{\rho_w}\right)^{1/2}.$$ (13)

The wind-induced surface drift currents at various fetches can now be determined from (3) and (13). Since the wind-stress coefficient decreases with increasing fetch (Wu, 1969a) and since the wind-induced surface drift current is proportional to the wind-friction velocity, the ratio between the wind-induced surface drift current and the wind velocity (V_n/U_z), as illustrated in Fig. 4, decreases with increasing fetch.

The Stokes surface transports can be obtained from (1) and (10) by

$$\frac{V_v}{U_z} = 0.0186(gLU_z^{-2})^{0.03}.$$ (14)

Lines representing this expression under various wind velocities at different fetches are shown in Fig. 4, indicating that due to the spatial wave growth with fetch the wave-induced drift current increases with fetch.

Combining wind- and wave-induced components, the ratio between the total surface-drift current and the reference wind velocity (V/U_z) is shown in Fig. 4 to decrease with increasing fetch at short fetches, and to be independent of fetch at long fetches. The total surface drift current is shown in the figure to be about 3.1% of the wind velocity at very long fetches.

3) COMPARISON OF PRESENT ESTIMATION WITH OTHER CALCULATIONS

Assuming that only wave components on the high-frequency side of the spectral peak contribute to the mass transport, Bye (1967) obtained from (5) and (6)

$$V_v = 2\beta g/\sigma_p,$$ (15)

in which σ_p is the frequency where the spectrum is peaked. The spectral coefficient β was considered to have a constant value of 0.015 in his estimate. Subsequently, Longuet-Higgins (1969) and Liu (1971) reported that the spectral coefficient actually decreases with increasing fetch; at very long fetches in the open sea, $\beta = 0.0137$ was suggested by Longuet-Higgins. For these fetches, the phase velocity of the wave component at the spectral peak is about the same as the wind velocity, $U = g/\sigma_p$. Consequently, we have from (15), $V_v/U = 2\beta = 0.0274$, which is in good agreement with the present estimates shown in Fig. 4. Recently, the spectral coefficient was found to decrease with increasing nondimensional fetch gLU_{10}^{-2}. In other words, for the same wind velocity, β decreases with increasing fetch; for the same fetch, β increases with wind velocity. Coupling these trends with (15) we see as illustrated in Fig. 4 that the mass transport at the sea surface decreases with fetch and increases with wind velocity.

A formula similar to (14) was proposed by Kondo (1976). The surface mass transports for $U_{10} = 10$ m s^{-1} at various fetches were calculated from Kondo's and the present expressions and are shown in Table 1. In comparison with the present as well as other results, such as those discussed above, Kondo's estimate is seen in the table to provide rather low values.

4) COMPARISON OF PRESENT ESTIMATION WITH OCEANIC MEASUREMENTS

The present estimation of surface drift currents does not take into consideration of Ekman boundary layer (Ekman, 1905), according to which the direction

TABLE 1. Ratios (%) between estimated surface mass transport and wind velocity.

Fetch (km)	10	50	100	500	1000	5000
Kondo (1976)	1.63	1.68	1.70	1.75	1.77	1.82
Equation (15)	2.29	2.40	2.45	2.57	2.63	2.95

of sea-surface currents deviates by 45° from the wind direction. Insignificant error, however, may result by this simplification. As pointed out recently by Madsen (1977), the angle between the surface drift current and the wind is only on the order of 10° or less, if a realistic model for the eddy viscosity is adopted. The actual eddy viscosity is believed to vary linearly with water depth, while a constant vertical eddy viscosity was assumed in Ekman's (1905) classical study. Furthermore, in a recent analysis of velocity records of drifters, Kirwan et al. (1979) concluded that a linear law relating the wind-induced surface drift current and the wind velocity was superior to the classic quadratic law leading to Ekman-type currents.

The drift currents at the sea surface were systematically measured by Hughes (1956) with plastic envelopes floating close to the water surface. He found that the water within 1 cm or so of the surface drifted parallel to the wind. The drifting speeds of plastic envelopes were averaged, and the ratio between the average drifting speed and the wind velocity was found to be 3.3%. This value agrees well with the present estimate shown in Fig. 4.

In another field observation, aerial photographs were taken of movements of oil spills from the *Torrey Canyon* (Smith, 1968). Successive positions of a large patch of oil were traced for a period of 15 days. The oil patch was found to drift in the direction of the wind and at 3.4% wind velocity. Again, the results are in good agreement with the present estimation. (As discussed later, the drift of a large oil patch should not differ significantly from the actual surface drift current.)

3. Drift currents of a slick surface

a. Various interactions between surface slick and wind waves

Quite often the sea surface is covered by either man-made or natural slicks. The slicks may be monolayers, which can effectively damp capillary waves (Barger et al., 1970; Hühnerfuss et al., 1981) due to a surface-tension gradient produced by passing waves. However, such a gradient generally may not be as strong with (crude) oil slicks, which therefore may not damp capillary waves as effectively as the monolayer. The sea surface becomes smoother with more damping of ripples; consequently, the wind stress, and therefore the wind-induced drift current, over a slick surface are smaller than those over a clean surface.

The inextensible slick at the water surface is also known (Phillips, 1977) to cause additional attenuation of long waves, and therefore of additional loss of wave momentum. This additional loss is supported entirely by the Reynolds stress just below the surface. A so-called surface streaming relative to the fluid below the boundary layer developed along the slick is

set up. In other words, the mass transport of a slick surface is relatively faster than that of a clean surface. This effect on the wave-induced drift current, which is increased due to the presence of a surface film, is opposite to that on a wind-induced drift current, which is reduced. It is also observed that effects of films on surface mass transport may be much stronger with oil slicks (Alofs and Reisbig, 1972) than with monolayers (Lange and Hühnerfuss, 1978).

b. Increase of mass transport due to films

1) ANALYTICAL CONSIDERATIONS

The rate of energy dissipation of deep-water waves per unit area of the water surface $\dot{E}_c$ can be shown as (Phillips, 1977)

$$\dot{E}_c = -2\mu_w\sigma^2a^2k, \tag{16}$$

where μ_w is the dynamic viscosity of water. With a densely packed surface film, the rate of energy dissipation of deep-water waves per unit water-surface area $\dot{E}_s$ becomes (Phillips, 1977)

$$\dot{E}_s = -\tfrac{1}{2}\mu_w\sigma^2a^2n, \tag{17}$$

where $n = (\sigma/2\nu_w)^{1/2}$, and ν_w is the kinematic viscosity of water.

A film causes much attenuation of wave amplitude but has negligible influence on wavelength. The rate of decrease of wave momentum $\Delta\dot{M}$ resulting from this additional energy dissipation of waves over a slick surface than over a clean surface can be expressed as

$$\Delta\dot{M} = (\dot{E}_s - \dot{E}_c)c^{-1} = -\mu_w\sigma^2a^2\left(\frac{n}{2} - 2k\right)c^{-1}. \tag{18}$$

A mean stress acting on a surface film in the direction of wave propagation is produced by this additional momentum flux. Consequently, the mass transport of waves at a slick surface is faster than that at a clean surface.

The wind-induced surface drift current has been related in (3) to the friction velocity of the aqueous boundary layer immediately below the air-water interface. Extending this result to the present case with the additional momentum flux due to a film, we can obtain the maximum possible "additional" surface drift current due to extra wave damping by a film from

$$V_s = 22\left(\frac{\Delta\dot{M}}{\rho_w}\right)^{1/2}. \tag{19}$$

The dissipation of wave energy per unit water-surface area due to the presence of a surface film increases with the size of the film, until the size of the film reaches the length of surface waves. In other words, the movement of a film along the direction of wave propagation should be faster than that of

water particles at a clean surface. The ratio between these two movements increases with the film length when the film length is shorter than the wavelength, and approaches asymptotically the maximum value when the film length approaches the wavelength.

2) EXPERIMENTAL RESULTS

Experiments have been conducted by Alofs and Reisbig (1972) to investigate wave-induced drifts of simulated oil slicks in a wave tank. Floats made of thin, flexible plastic sheets of various sizes were carefully laid on the water surface before the experiment, and were found to conform to the wavy surface. The drift of floats due to waves, verified to be very similar to that of an oil lens, was measured with mechanically generated waves of two different lengths: $\lambda = 25.4$ and 50.8 cm; the wave height was also varied to provide various wave steepnesses. The experimental results of Alofs and Reisbig are replotted in Fig. 5a, where V_f is the float velocity and l the float length. Lines are drawn in the figure to illustrate trends of

the data: 1) the measured velocity of the float is always greater than the calculated Stokes surface transport of waves, not shown in the figure; 2) the float velocity for a given wave condition increases with the float length, and approaches asymptotically an equilibrium value; 3) over shorter waves, the float velocity tends to reach the equilibrium value earlier with a shorter float.

3) FURTHER ANALYSIS OF EXPERIMENTAL RESULTS

For each experimental condition, we obtain from Fig. 5a an equilibrium drift velocity V_{max}, at which drift current no longer increases with float length. Inasmuch as the mass transport over a clean surface in Alofs and Reisbig's experiments was found to be greater than V_v, we choose to determine the additional movement due to the presence of a float from $V_{max} - V_{l=0}$, where $V_{l=0}$ is the velocity of the "float" of zero length found by extending their results to $l = 0$.

As discussed earlier, the differential drift between slick and clean surfaces increases with film length, and the maximum difference is produced by a film with a length approaching the wavelength. Consequently, the ratio between the measured and the maximum differential drifts is plotted in Fig. 5b versus the ratio between float length and wavelength. It is illustrated in this nondimensional plot that all of the data follow the same trend. In other words, the movements of floats of different lengths over waves of not only various steepnesses but also various lengths can be incorporated by a nondimensional relation represented by the straight line fitted to the data and expressed as

$$\left.\begin{array}{ll} \dfrac{(V_f - V_{l=0})}{(V_{max} - V_{l=0})} = 1 - \left(\dfrac{3}{4}\right)\log\left(\dfrac{l}{\lambda}\right), & \text{for} \quad l/\lambda < 1 \\[4mm] \dfrac{(V_f - V_{l=0})}{(V_{max} - V_{l=0})} = 1, & \text{for} \quad l/\lambda > 1 \end{array}\right\} ,$$

$$(20)$$

where V_{max} can be calculated from (21), discussed as follows.

The drift of surface floats used here was shown by Alofs and Reisbig (1972) to be very similar to that of oil films. If we consider that the interaction between surface floats and waves is also similar to that between films and waves, we can relate additional drifts introduced by a float, $V_{max} - V_n$ and $V_{max} - V_{l=0}$, to the additional momentum flux from waves to film, $\Delta \dot{M}/\rho_w$. The results, obtained from (19) and shown in Fig. 6, are very much scattered but confirm roughly the mechanism discussed in the previous section. A straight line passing through the origin is fitted to each set of data
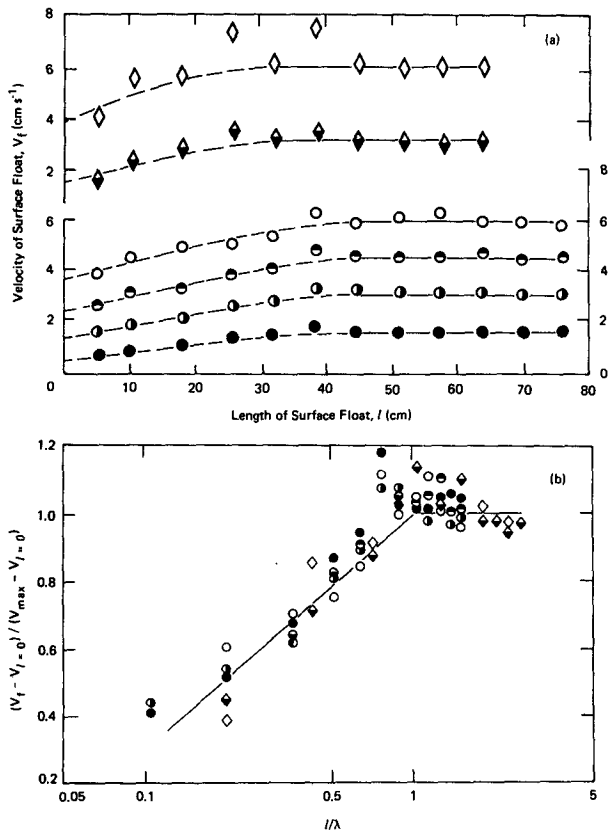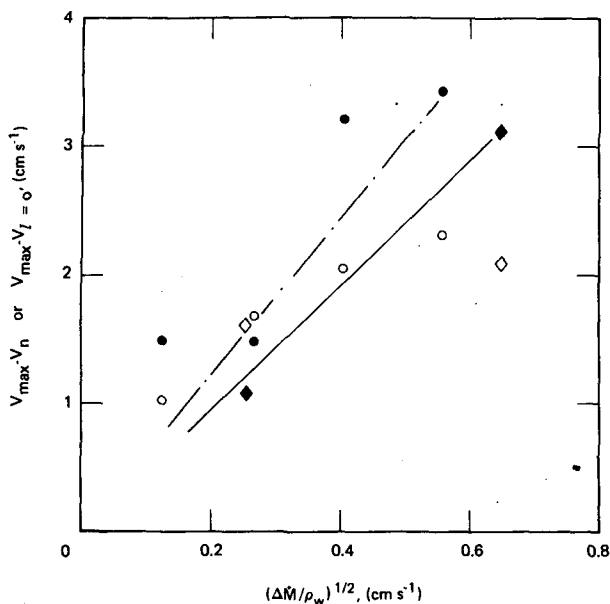
FIG. 5. Motions of surface floats of various sizes over waves. (a) Experimental results of Alofs and Reisbig (1972) and (b) additional surface mass transport due to wave damping by film. The experimental conditions are: $\lambda = 25.4$ cm, $a/\lambda = 0.138$ (diamond) and 0.054 (half solid diamond); $\lambda = 50.8$ cm, $a/\lambda = 0.108$ (open circle), 0.078 (top half solid), 0.054 (right half solid) and 0.024 (solid circle).

FIG. 6. Wave attenuation and mass transport. The open symbols and dot-dash line are results related to V_n and the solid symbols and solid line related to $V_{l=0}$; the diamonds are results obtained with $\lambda = 25.4$ cm and the circles with $\lambda = 50.8$ cm.

$$\left.\begin{aligned}\frac{(V_{max} - V_{l=0})}{(\Delta \dot{M}/\rho_w)^{1/2}} &= 4.8 \\[2mm] \frac{(V_{max} - V_n)}{(\Delta \dot{M}/\rho_w)^{1/2}} &= 6.1\end{aligned}\right\} \quad . \tag{21}$$

Both values on the right-hand side of (21) are much smaller than the maximum possible value of 22 shown in (19), the efficiency of the momentum transport from wave damping to the surface drift current is then only about 25%.

4) DIFFERENT EFFECTS ON MONOLAYER AND OIL SLICK

The floats of monolayers were used by Lange and Hühnerfuss (1978) in their experiments. The floats were longer than the length of waves tested (20 cm $< \lambda < 70$ cm). They found no streaming effects, as the drift velocity of floats compared well with the Stokes surface transport. This may be due to that monolayers are much more extensible than oil slicks.

c. Decrease of wind-induced surface drift current due to film

Effects of the monolayer upon the wind structure have been studied by Barger et al. (1970). The monolayer was generated by a spontaneous spreading of a film-forming oleyl alcohol on the sea surface. Vertical wind profiles over clean and slick surfaces were verified to follow the logarithmic law

$$\frac{U_z}{u_{*_a}} = \frac{1}{\kappa} \ln\left(\frac{z}{z_0}\right), \tag{22}$$

where κ is the Karman universal constant, and z_0 the roughness length. Values of z_0 and u_{*_a} for both surfaces are presented in Fig. 7a, b.

It is seen in Fig. 7a that over a clean surface the roughness length increases sharply at a wind velocity of approximately 2 m s^{-1}. This sharp increase is believed to be due to a rapid growth of small waves around this velocity, where the transition of the airflow boundary layer from smooth to rough presumably took place. The presence of a monolayer causes damping of small waves; consequently, the roughness length was drastically reduced. The transition of the airflow boundary layer, therefore, occurred at a higher wind velocity with the stem of the roughness-length growth shifting to a higher wind velocity of approximately 6 m s^{-1}. Below this wind velocity, the sea surface is smooth; above this velocity, the roughness length of a slick surface is about the same as that of
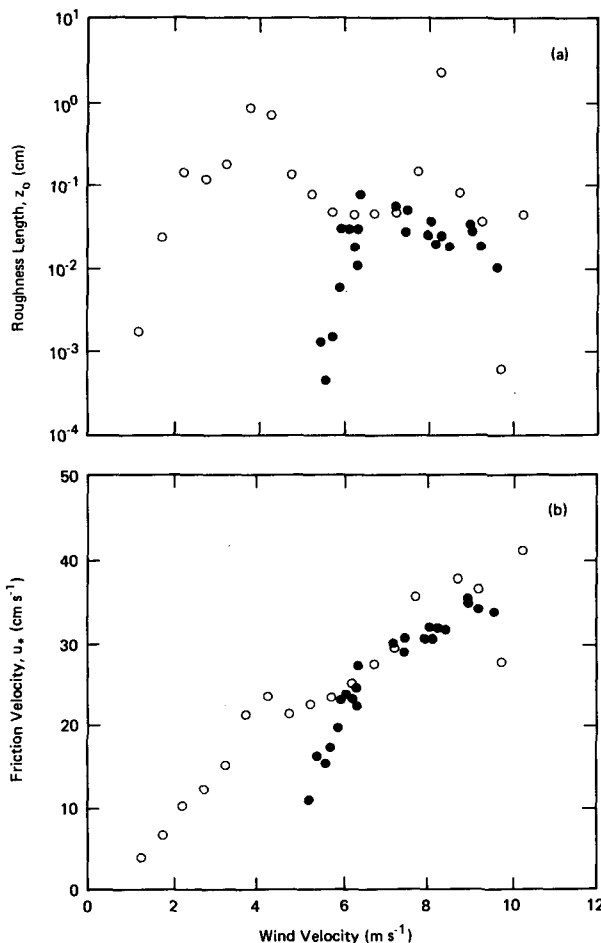

FIG. 7. Roughness lengths (a) and wind-friction velocities (b) over clean (open circle) and slick (solid circle) sea surfaces.

a clean surface. The similarity in roughness lengths for clean and slick surfaces at high wind velocities is probably due to disruption of the surface film by wind.

Similar features are illustrated by the wind-friction velocity shown in Fig. 7b. Before the disruption of the monolayer, the wind velocity for a surface covered with a monolayer is about twice that for a clean surface having the same friction velocity. Because the wind-induced drift current is proportional to the wind-friction velocity, the ratio between the wind-induced surface drift current and the wind velocity for a slick surface is, therefore, about one half that for a clean surface.

No similar study as discussed above has been reported with wind blowing over a water surface covered by oil slicks.

4. Discussion

a. Components of surface drift currents and their superposition

Those dealing with field conditions (Bye, 1967; Kenyon, 1969) often considered that the drift current of the sea surface consisted of mainly the mass transport of waves, while those performing laboratory experiments (Shemdin, 1972) regarded that the surface drift current consisted of mainly the shear current induced by the wind. As discussed earlier (Wu, 1975) and illustrated in Fig. 4a, the major component of the surface drift current in the field is indeed the Stokes mass transport, and in the laboratory the wind-induced shear current. However, the other component in each group is always significant and cannot be neglected.

Both field and laboratory results also indicated that the measured total surface drift current was approximately independent of fetch. On the belief that the surface drift current consists mainly of only one component, an erroneous consideration may be advanced that both the Stokes mass transport and the wind-induced shear current are independent of fetch. Lange and Hühnerfuss (1978) reported that the mass transport comprised 25–30% of the total surface drift in both laboratory tanks and the field. As pointed out earlier (Wu, 1975) and shown in Fig. 4, each of the components depends rather strongly on, but varies differently with, the fetch. The total surface drift current, which is the sum of two components and is also the measured value, is approximately independent of fetch.

Lange and Hühnerfuss (1978) conducted a series of experiments, first with either wind or mechanically generated waves, and then with wind of the same velocity blowing over the same mechanical waves. The measured surface drift currents with both wind and mechanical waves were found to be different

from the sum of the currents with either wind or mechanical waves. On the basis of these results, they suggested that the effects of wind and waves cannot be simply superimposed. It should be pointed out, however, that even for the same wind velocity, the wind-friction velocities differ for the cases with and without pre-existing waves (Wu, 1977). Consequently, the wind-induced surface drift currents with pre-existing waves, being proportional to the wind-friction velocity, should not be the same as those without. Moreover, the Stokes mass transport also changes, as the resultant waves under wind differ significantly from pre-existing waves.

b. Direct illustration of wave drag

Following Stewart's (1961) proposal, evidences of the wave drag were provided, among others, by Dobson (1971), Hasselmann et al. (1973), and Wu (1975). Indications of the existence of wave drag can actually be found, however, even before Stewart's proposal. The setups and the drift currents of both wavy and waveless water surfaces under wind were measured in a laboratory tank (Keulegan, 1951) and an artificial pond (van Dorn, 1953). The wave suppression for the waveless case was achieved by adding either soap or detergent to the water surface. Their results are shown in Fig. 8a, c, where $R_d = VD/\nu_w$ is the depth Reynolds number with D being the water depth.

The water-surface setup in the presence of waves was found by Keulegan and van Dorn to be greater than that in the absence of waves; see Fig. 8b, d, where s is the water-surface setup. The difference in the
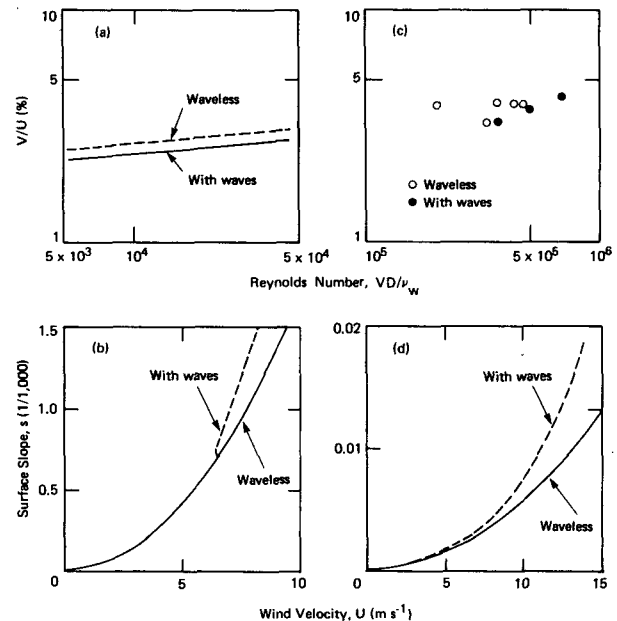

Fig. 8. Previous results from Keulegan (1951): (a) and (b), and from van Dorn (1953): (c) and (d).

magnitude of setups in these two sets of data is mainly due to the difference in water depth. The additional setup due to waves shown in Fig. 8b, d is in line with the consideration that a wavy surface is much rougher aerodynamically than a calm surface. Consequently, the wind-stress coefficient should be greater for a wavy than for a waveless surface. The ratio between surface drift current and wind velocity obtained by Keulegan with a calm surface, shown in Fig. 8a (where the lines fitted very closely to his data are reproduced), is about 7-8% greater than that with a wavy surface. The same trend is seen in van Dorn's data, shown in Fig. 8b, obtained under these two conditions. These results were considered surprising with the presence of waves causing an increase of the surface setup but a decrease of the ratio between surface drift current and wind velocity. As discussed earlier, the wind-induced drift current was found to be proportional to the wind-friction velocity. Therefore, the wind-induced current should be greater for a wavy surface, which being rougher has a larger set-up. Furthermore, the wave-induced current, the Stokes mass transport, is present over the wavy surface and is absent over the waveless surface. Reasoning solely from these arguments, it appears that the ratio between the total surface drift current and the wind velocity should be greater with than without presence of waves.

The above discrepancy suggested a reduction of the momentum flux from wind to currents, implying that a portion of the momentum flux from the wind is directly extracted by waves. Interpreting the concept of wave drag (Stewart, 1961), the momentum flux introduced by the wind is consumed mainly on producing currents in the absence of waves, while only a fraction of this flux is consumed for producing currents in the presence of waves. Considering that as discussed earlier the wave-induced currents are small in Keulegan and van Dorn's experiments conducted at short fetches and that the difference in wind-friction velocities for wave and for waveless surfaces is also small, the presence of the wave drag in the wavy case and its absence in the waveless case result in having a greater surface drift current at a waveless than at a wavy surface.

c. Effects of water depth on surface drift currents in contained bodies of water

Effects of water depth on surface drift currents have been studied much earlier by Keulegan (1951) and recently by Kondo (1976) and Spillane and Hess (1978). Among them, Keulegan provided the most proper (nondimensional) presentation as well as the most comprehensive set of data illustrating these effects. He related the ratio between surface drift current and wind velocity (V/U) to the depth Reynolds number R_d defined earlier. The ratio V/U was shown

to increase with R_d rapidly when $R_d < 10^3$ and gradually when $R_d > 10^3$, and tended to approach a constant at a higher R_d, say $R_d = 10^5$.

According to Keulegan's results, the surface drift currents in the field, because of its large depth Reynolds number, should not be affected by the water depth except at very low wind velocities. This is also evident from the field results compiled by Kondo (1976): one group with $D < 3.4$ m and the other with $D > 20$ m; there was no difference between these two groups of results. Some differences were shown for two groups of laboratory results—$D \leqslant 30$ cm and 30 cm $< D < 200$ cm—first by Kondo (1976) and again by Spillane and Hess (1978). The arbitrary division of the data by $D = 30$ cm may hinder illustrations of depth effects at shallow depths, and of lacking depth effects at large depths. In any event, the effects of water depth on surface drift currents, if there are still any, at those deep depths in the field discussed by Spillane and Hess should be negligible.

Assuming that both shear stress and roughness length are the same above and below the air–water interface, Spillane and Hess obtained an expression to show the variation of the ratio V/u_{*_w} with the water depth. The weak effects of water depth can easily be caused by their assumptions.

REFERENCES

Alofs, D. J., and R. L. Reisbig, 1972: An experimental evaluation of oil slick movement caused by waves. *J. Phys. Oceanogr.,* **2,** 439–443.

Baines, W. D., and D. J. Knapp, 1965: Wind driven water currents. *J. Hydraul. Div., ASCE,* **91,** 205–221.

Barger, W. R., W. D. Garrett, E. L. Mollo-Christensen and K. W. Ruggles, 1970: Effects of an artificial sea slick upon the atmosphere and the ocean. *J. Appl. Meteor.,* **9,** 396–400.

Bye, J. A. T., 1967: The wave drift current. *J. Mar. Res.,* **25,** 95–102.

Dobson, F. W., 1971: Measurements of atmospheric pressure of wind-generated sea waves. *J. Fluid Mech.,* **48,** 91–127.

Ekman, V. W., 1905: On the influence of earth's rotation on ocean currents. *Ark. Mat. Astron. Fys.,* **2,** 1–53.

Hasselmann, K., D. B. Ross, P. Müller and W. Sell, 1976: A parametric wave prediction model. *J. Phys. Oceanogr.,* **6,** 200–228.

Hughes, P., 1956: A determination of the relation between wind and sea-surface drift. *Quart. J. Roy. Meteor. Soc.,* **82,** 494–502.

Hühnerfuss, H., W. Alpers, W. L. Jones, P. A. Lange and K. Richter, 1981: The damping of ocean surface waves by a monomolecular film measured by wave staffs and microwave radars. *J. Geophys. Res.,* **86,** 429–438.

Kenyon, K. E., 1969: Stokes drift for random gravity waves. *J. Geophys. Res.,* **74,** 6991–6994.

Keulegan, G. H., 1951: Wind tides in small closed channels. *J. Res., Nat. Bur. Stand.,* **46,** 358–381.

Kirwan, A. D., Jr., G. McNally, S. Pazan and R. Wert, 1979:

Analysis of surface current response to wind. *J. Phys. Oceanogr.*, **9**, 401–412.

Kondo, J., 1976: Parameterization of turbulent transport in the top meter of the ocean. *J. Phys. Oceanogr.*, **6**, 712–720.

Lange, P., and H. Hühnerfuss, 1978: Drift response of monomolecular slicks to wave and wind action. *J. Phys. Oceanogr.*, **8**, 142–150.

Lighthill, M. J., 1971: Time-varying currents. *Phil. Trans. Roy. Soc. London,* **A270**, 371–390.

Liu, P. C., 1971: Normalized and equilibrium spectra of wind waves in Lake Michigan. *J. Phys. Oceanogr.*, **1**, 249–257.

Longuet–Higgins, M. S., 1969: On wave breaking and the equilibrium spectrum of wind-generated waves. *Proc. Roy. Soc. London,* **A310**, 151–159.

Madsen, O. S., 1977: A realistic model of the wind-induced Ekman boundary layer. *J. Phys. Oceanogr.*, **7**, 248–255.

Phillips, O. M., 1977: *The Dynamics of the Upper Ocean,* 2nd ed. Cambridge University Press, 336 pp.

Shemdin, O. H., 1972: Wind-generated current and phase speed of wind waves. *J. Phys. Oceanogr.*, **2**, 411–419.

Smith, J. E. (Ed.), 1968: *"Torrey Canyon" Pollution and Marine Life.* Cambridge University Press, 196 pp.

Spillane, K. T., and G. D. Hess, 1978: Wind-induced drift in contained body of water. *J. Phys. Oceanogr.*, **8**, 930–935.

Stewart, R. W., 1961: The wave drag of wind over water. *J. Fluid Mech.*, **10**, 189–194.

Stokes, G. G., 1847: On the theory of oscillating waves. *Trans. Cambridge Phil. Soc.*, **8**, 441–445.

van Dorn, W. G., 1953: Wind stress on an artificial pond. *J. Mar. Res.*, **12**, 249–276.

Wiegel, R. L., 1964: *Oceanographical Engineering.* Prentice-Hall.

Wu, Jin, 1968: Laboratory studies of wind-wave interactions. *J. Fluid Mech.*, **34**, 91–112.

——, 1969a: Froude number scaling of wind-stress coefficients. *J. Atmos. Sci.*, **26**, 408–413.

——, 1969b: Wind stress and surface roughness at air–sea interface. *J. Geophys. Res.*, **74**, 444–455.

——, 1971: Anemometer height in Froude scaling of wind stress. *J. Waterways Harbors Coastal Eng. Div., ASCE,* **97**, 131–137.

——, 1973: Prediction of near-surface drift currents from wind velocity. *J. Hydraul. Div., ASCE,* **99**, 1291–1302.

——, 1975: Wind-induced drift currents. *J. Fluid Mech.*, **68**, 49–70.

——, 1977: Effects of long waves on wind boundary layer and on ripple slope statistics. *J. Geophys. Res.*, **82**, 1359–1362.

——, 1980: Wind-stress coefficients over sea surface near neutral conditions—A revisit. *J. Phys. Oceanogr.*, **10**, 727–740.